PHYSICAL REVIEW B VOLUME 24, NUMBER 6 15 SEPTEMBER 1981

First-principles electronic structure of Si, Ge, GaP, GaAs, ZnS, and ZnSe. II. Optical properties

C. S. Wang
Department of Physics and Astronomy, University of Maryland, College Park, Maryland 20742 and Naval Research Laboratory, Washington, D. C. 20375

B. M. Klein
Naval Research Laboratory, Washington, D. C. 20375

(Received 18 March 1981)

The interband optical properties of Si, Ge, GaP, GaAs, ZnS, and ZnSe were calculated using *ab initio* self-consistent energy bands and wave functions obtained from the previous paper (paper I). Qualitatively good agreement with experiment is found, but all peak positions are shifted to lower energies since the local-density approximation underestimates the optical band gaps. Agreement with experiment with regard to line shape and peak position can be improved using an empirical energy-dependent self-energy correction as appears in the Sham-Kohn local-density theory of excitation. After examining the possible effects of lifetime broadening, our results indicate that additional many-body, excitonic, and local-field corrections must be included to achieve quantitative agreement in the intensity of certain features in the optical spectra.

I. INTRODUCTION

The optical properties of the diamond and zinc-blende semiconductors have been the subject of intense investigations for many years. Surprisingly, experiments showed similar qualitative results among the group IV, III-V, and II-VI semiconductors, with the imaginary part of the dielectric constants (ϵ_2) exhibiting two major peaks.[1-3] The first structure has been attributed to the $M0$- or $M1$-type critical-point transition, and the second one to the $M2$ type. Earlier theoretical efforts employing the empirical pseudopotential method adjusted the model pseudopotentials to fit either the experimental data[4-8] or empirically refined OPW energy bands.[9-10] In general, the optical spectra calculated using the resulting pseudoenergies and wave functions within the one-electron approximation underestimate the intensity of the observed $E1$ peak in ϵ_2 by as much as 50% while the $E2$ peak is overestimated. The theoretical ϵ_2 remains larger than the measurement until around 6–8 eV, and beyond this point the theoretical values become increasingly too small. This gives rise to theoretical results for reflectivity and energy-loss spectrum intensities more than twice as large as experiment at high energies.

In an effort to understand some of these discrepancies, Louie *et al.*[7] have calculated the dielectric response matrix in order to investigate the possible local-field corrections to the optical spectrum of Si. They found that the prominent peak positions are not altered, even though the overall strength of ϵ_2 below 7 eV is reduced, contrary to what is required to reconcile theory with experiment for the $E1$ and $E2$ structure. However, significant improvements arising from the local-field corrections are found at higher energies where the energy-loss spectrum shows the most dramatic effect. The theoretical intensity of the plasmon peak at 18 eV is reduced by 50%, significantly improving the agreement with experiment. Presumably better values of ϵ_2 in this energy region will also reduce the discrepancy in the reflectance spectrum.

The existence of contributions from the metastable continuum-exciton to the $E1$ structure in $\epsilon_2(\omega)$ for the diamond and zinc-blende semiconductors has been suggested by several authors.[11-16] It was Phillips[11] who first proposed the effect of the hyperbolic exciton on the $M1$-type van Hove singularity structure. Using the tight-binding model with an on-site contact interaction to approximate the Coulomb interaction between the electron and the hole, Velicky and Sak[12] have demonstrated that the

$M0$ and $M1$ branch points of ϵ_2 were enhanced and sharpened, while the $M2$ and $M3$ branch points were weakened and smoothed out. Experimentally, it was found that the temperature[13] and pressure[14] dependence of the line shape or the symmetry[15] in the wavelength modulation reflectance spectra cannot be explained without introducing excitonic effects.

More recently, Hanke and Sham[16] have included many-body effects in a calculation of the dielectric response of Si which take into account both the screened electron-hole attraction (the excitonic effect) and the local-field effect. In good agreement with Louie *et al.*[7] they found the local-field effect alone shifts the oscillator strength to higher energy and furthers the discrepancy with the experiments at low energies. When both excitonic and local-field corrections are included, the intensity of the $E1$ peak is almost doubled at the expense of their higher energy counterparts. Furthermore, the position of the $E1$ peak is lowered by 0.2 eV and the static dielectric constant $\epsilon_1(0)$ is raised from 9.85 to 10.4. The experimental value is 11.7. Thus, the overall agreement with the experiment is significantly improved. However, such a detailed quantitative account of various many-body effects may be limited by the choice of the starting one-electron energy bands. Quantitatively, there are substantial differences in ϵ_2 calculated within the one-electron picture between Hanke and Sham[16] and that of Louie *et al.*[7] Since the pseudopotential energies used by Louie *et al.* were adjusted to reproduce the optical data, all major structures in their ϵ_2 coincide with the experiments. On the other hand, Hanke and Sham[16] showed that the onset of the ϵ_2 spectrum calculated from their energy bands is shifted to higher energy by more than 0.2 eV compared with the experiment. This is contrary to the results of self-consistent energy-band calculations within the local-density-functional formalism (see I), where the optical band gaps are always underestimated. The intensity distribution of their uncorrected theoretical ϵ_2 appears to be quite different too. Louie *et al.*[7] found ϵ_2 greater than experiment beginning at the maximum of the $E2$ peak (4.2 eV) until approximately 9 eV, where the theory crosses the experiment.[1] In Hanke and Sham's results[16] the ϵ_2 intensity remains smaller than experiment until 6 eV. Since this is beyond the two prominent peaks, the theory must remain above the experiment over a fairly large energy range in order to satisfy the f-sum rule. The corresponding reflectivity and energy-loss spectrum would be affected accordingly.

The purpose of the present paper then is to provide an accurate *ab initio* description of the optical spectrum within the one-electron picture for a number of these semiconductors. The energies and wave functions used are determined self-consistently within the local-density-functional formalism[17–18] without any shape approximation or adjustable fitting parameters. The only experimental input is the lattice constant. It has been gradually established that band theory using the same exchange and correlation potential can provide a rather consistent, method-independent band structure if the charge density is evaluated self-consistently. It is also of interest to compare our results with previous studies using pseudo wave functions which represent only the smooth part of the wave function without the core contribution.

II. METHOD

In the previous paper, we have investigated the ground-state properties of Si, Ge, GaP, GaAs, ZnS, and ZnSe using the self-consistent linear combination of Gaussian orbitals (LCGO) method[19] and the local-density exchange potential of Kohn-Sham[18] with the correlation potential of Wigner.[20] Relativistic effects were neglected. The LCGO basis set consists of minimum atomic orbitals augmented by an additional s, p, and d shell of virtual orbitals for added variational flexibility. The crystal potential is expressed as a superposition of spherical Gaussian orbitals centered at each atomic site, plus a Fourier series expansion to accurately describe the bonding character in the tetrahedral environment. Self-consistency is obtained iteratively based on ten special $\vec{k}$ points of Chadi and Cohen[21] in the $\frac{1}{48}$th of the Brillouin zone. The self-consistent energies and wave functions are used here to study the optical properties of the six semiconductors.

The frequency-dependent dielectric function within the one-electron picture is given by the standard formula

$$\epsilon(\omega)=1-\frac{2e^2}{m^2\pi^2}\sum_{n,l}\int d^3k\frac{f_n(\vec{k})[1-f_l(\vec{k})]\,|\langle n\vec{k}\,|\,\vec{p}\,|\,l\vec{k}\rangle|^2}{\hbar\omega_{nl}(\vec{k})[\hbar\omega-\hbar\omega_{nl}(\vec{k})+i/\tau][\hbar\omega+\hbar\omega_{nl}(\vec{k})+i/\tau]}\,, \tag{1}$$

where the quantitiy $f_n(\vec{k})$ is the zero-temperature Fermi distribution function for band index n and wave vector $\vec{k}$, and $\hbar\omega_{nl}(\vec{k})=E_n(\vec{k})-E_l(\vec{k})$ is the energy difference. We have included a factor of 2 for spin, and a phenomenological relaxation time, τ, to describe the lifetime-broadening effects. The remaining notation is conventional. Because we have used a basis set of Gaussian orbitals, the wave-vector-dependent momentum matrix elements $\langle n\vec{k}\,|\,\vec{p}\,|\,l\vec{k}\rangle$ can be evaluated analytically. Initially, ϵ_2 is calculated in the sharp limit ($\tau\rightarrow\infty$) at energies between 0 and 29 eV. All valence and conduction states which lie within this interband transition range have been included. The Brillouin zone integration is calculated numerically by the linear analytical tetrahedron method[22] based on 89 $\vec{k}$ points in the $\frac{1}{48}$th irreducible wedge. Once the imaginary part of the dielectric constant has been evaluated, the real part may be calculated by the Kramers-Kronig transformation. To check the convergence, we have attached a tail function of the form $\epsilon_2(\omega)=\beta\omega/(\omega^2+\gamma^2)^2$ for energies greater than 29 eV. For a choice of $\gamma=4.5$ eV and β determined by the continuity of ϵ_2 at 29 eV, no noticeable differences were found in $\epsilon_1(\omega)$ in the energy range of interest.

In the present work we have investigated empirically an energy-dependent self-energy correction to the optical spectrum of these semiconductors through a procedure introduced for metals by Janak *et al.* in a study of the optical conductivity of Cu.[23] As Sham and Kohn[24] have shown, the application of the self-consistent ground-state energies to the excitation spectrum requires a self-energy correction. For slowly varying density the corrected excited-state energy $\tilde{E}_n(\vec{k})$ near the Fermi energy E_F can be obtained from the ground-state energy $E_n(\vec{k})$ by

$$\tilde{E}_n(\vec{k})=E_n(\vec{k})+\lambda_n(\vec{k})[E_n(\vec{k})-E_F]\,, \tag{2}$$

with

$$\lambda_n(\vec{k})=\frac{\int d^3r\,|\,\psi_n(\vec{k},\vec{r})\,|^2[1-m^*(\rho(\vec{r}))]}{\int d^3r\,|\,\psi_n(\vec{k},\vec{r})\,|^2 m^*(\rho(\vec{r}))}\,. \tag{3}$$

Here $m^*(\rho(r))$ is the effective mass for the interacting electron gas evaluated for a ground-state charge density ρ, and $\psi_n(\vec{k},\vec{r})$ is the ground-state wave function. In the present study $\lambda_n(\vec{k})$ is assumed to be independent of n and $\vec{k}$ and is adjusted empirically to fit the experimentally observed optical transition energies. Janak *et al.*[23] have shown that such an approximation leads to an energy-dependent but space-independent excited-state exchange and correlation potential, and there is no change in the ground-state wave functions and momentum matrix elements. Furthermore, the revised imaginary part of the dielectric constant $\tilde{\epsilon}_2(\omega)$ is given by

$$\tilde{\epsilon}_2(\omega)=\frac{1}{1+\lambda}\epsilon_2\left[\frac{\omega}{1+\lambda}\right]. \tag{4}$$

Both the self-energy corrections described here and the continuum-exciton effect discussed in Sec. I arise from the interaction between the excited electron and the screened hole left behind, but with rather different consequences. The self-energy corrections amount to the additional energy needed to pull the electron and the hole apart during the transition from the initial to the final state while the system relaxes, with the transition energy being increased from the one-electron value. However, in the case of semiconductors the relaxation may be so slow that the electron being excited to the final state still feels the Coulomb attraction of the partially screened hole after making the transition. Thus, the final-state energy, and hence, the transition energy are reduced from the fully relaxed value. Note that the second effect due to the continuum exciton was not included explicitly in Eq. (4) and its effect on the intensity of the $E1$ peak was neglected. It is also known that the effects of the exchange and correlation corrections become negligible at sufficiently high energy,[25] so we expect Eq. (4) to fail for large ω. Nevertheless, it is interesting to see how several of the optical transition energies calculated within the local-density approximation can be improved using only one adjustable parameter, λ. The remaining differences between our results and experiment are an indication of the magnitude of the other many-body effects. By presenting results determined in a systematic way for a number of these materials it is our hope to stimulate more work in the search for an improved *ab initio* theory for describing the optical spectra of semiconductors.

III. RESULTS AND DISCUSSION

A. $\epsilon_2(\omega)$

The imaginary parts of the dielectric constants between 0 and 12 eV are shown in Figs. 1, where they are compared with the experimental measurements (dashed lines) of Philipp and Ehrenreich[1] for Ge, Si, GaAs, GaP, of Cardona and Harbeke[2] for ZnS, and of Freeouf[3] for ZnSe. The dotted lines are theoretical results due to interband transitions in the sharp limit ($1/\tau=0$) while the solid lines include

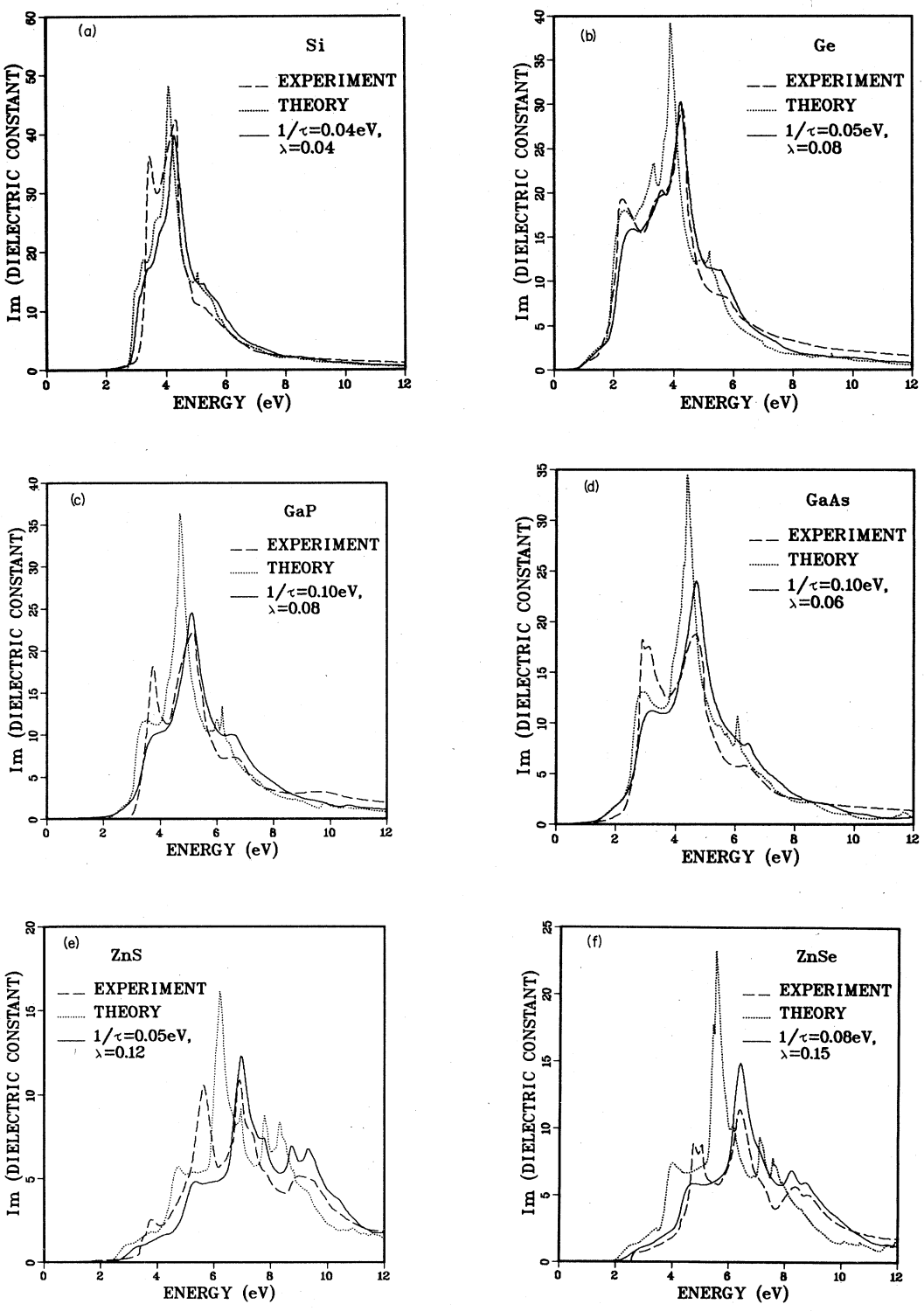

FIG. 1. Imaginary part of the dielectric constant. The experimental results (dashed lines) are from Ref. 1 for Ge, Si, GaP, and GaAs, Ref. 2 for ZnS, and Ref. 3 for ZnSe. The dotted lines are interband contributions to Eq. (1), while the solid lines include additional lifetime-broadening and self-energy corrections as indicated in each figure and discussed in the text.

the effects of the lifetime-broadening and self-energy correction as described in Sec. II. The effect of the relaxation time τ is equivalent to a Lorentzian broadening. The value of τ indicated in each figure was chosen empirically to reproduce the width of the experimentally measured peaks, while the self-energy parameter λ, also shown, was chosen so as to align the optical transition energies.

In general, our calculated values of $\epsilon_2(\omega)$ are in good qualitative agreement with experiment although we find that the one-electron local-density approximation consistently underestimates the optical band gaps such that all theoretical peak positions in $\epsilon_2(\omega)$ (dotted lines) are shifted to lower energy with respect to the experiments (dashed lines). The inclusion of empirical lifetime and self-energy corrections improves the theoretical-experimental comparison. In good agreement with previous findings,[4-10] the theory tends to underestimate the intensity of the $E1$ peak while the $E2$ peak is overestimated. Excitonic effects must be included to achieve better quantitative agreement with experiment. The self-energy parameter λ needed to reproduce the experimental optical transition energies, Si(0.04), Ge(0.08), GaP(0.08), GaAs(0.06), ZnS(0.12), and ZnSe(0.15), appears to increase with increasing ionicity and decreasing covalency, the major deviation being GaAs. Similar trends can be seen in the ratio of the experimental oscillator strength between the $E1$ and $E2$ peaks within each group which may be considered as an indirect measure of excitonic effects: Ge is smaller than Si, and ZnSe is smaller than ZnS, but GaAs is larger than GaP. Obviously these features are sensitive to the details of the electronic structure.

We have determined the regions in the Brillouin zone which give rise to a large contribution to $\epsilon_2(\omega)$ by examining the wave-vector-dependent momentum matrix elements. They are discussed separately for each material. Note that the reader should refer to Figs. 1—6 of paper I for the energy bands referred to in the following discussion.

1. Germanium

The imaginary part of the dielectric constant of Ge is shown in the upper right panel of Fig. 1. We shall first consider the dotted line which represents the interband transition with no modification due to lifetime or other self-energy corrections. The onset of the absorption edge in ϵ_2 occurs at 0.72 eV, which corresponds to the direct optical band gap $\Gamma^v_{25'}+\Gamma^c_{2'}$. Up to approximately a quarter of the way from Γ to L along the Λ direction the conduction band rises sharply to yield a gap of 1.9 eV, where it begins to be parallel to the top of the valence band until the L point. This explains the drastic increase in the slope of ϵ_2 beginning at 1.9 eV. However, no critical-point structure can be identified with the $L^v_{3'}\rightarrow L^c_1$ transition at 1.92 eV. Two small structures are found at 2.36 and 3.35 eV before the main peak at 3.9 eV, followed by a shoulder at 5.20 eV. The first structure at 2.36 eV is attributed to regions in the Brillouin zone extending from $\Lambda^v_3\rightarrow\Lambda^c_1$ near L, to $\Sigma^v_2\rightarrow\Sigma^c_3$ near Γ. The second peak at 3.35 eV arises mainly from the region surrounding Γ ($\Gamma^v_{25'}\rightarrow\Gamma^c_{15}$), especially along the Δ direction, where the valence and conduction bands remain parallel to each other until three-fourths of the distance to X. Both volume effects and van Hove singularities are important in order to account for the major structure at 3.9 eV. Contributions arise mainly from the outer portions of the Brillouin zone, particularly between the Δ and Σ directions, including the critical points $X^v_4\rightarrow X^c_1$ (3.91 eV), which is almost degenerate with $K^v_2\rightarrow K^c_3$ (3.87 eV). Finally, the shoulder at 5.20 eV is attributed to the transition $\Lambda^v_3\rightarrow\Lambda^c_3$ towards L, and $\Delta^v_5\rightarrow\Delta^c_{2'}$ midway between Γ and X, with the small but sharp structure at 5.20 eV coinciding with the $L^v_3\rightarrow L^c_3$ transition.

The solid line in the Ge panel of Fig. 1 shows the theoretical results including lifetime-broadening ($1/\tau=0.05$ eV) and self-energy corrections ($\lambda=0.08$) for Ge. The λ value was chosen to align the main $E2$ peak with the experiment,[1] while $1/\tau$ was chosen to reproduce the corresponding experimental width. Note that significant improvements were also found in the position of the shoulders on both sides of the main peak. The $E1$ peak at 2.36 eV is shifted away from experiment to higher energy. This is to be expected because the excitonic effect, not included in the present calculation, will lower the transition energy as well as enhance its oscillator strength. Beyond the main $E2$ peak, the theoretical intensity is higher than experiment until approximately 6.4 eV, where the two curves cross each other. Similar results for Si in the high-energy region were reported by Louie *et al.*,[7] where agreement with experiment was improved after including the local-field effect.

2. Silicon

In contrast to Ge, where the transition along Λ and Δ are well separated in the ϵ_2 spectrum by 1

eV, these two structures are not resolved in Si. However, several structures have been reported near the absorption edge of the modulation spectrum of Si and a precise identification of the corresponding transitions is still in question.[4] Our results (dotted line, with no modification due to lifetime or other self-energy corrections) show that the onset of ϵ_2 occurs at 2.66 eV which corresponds to the transition $\Gamma^v_{25'} \rightarrow \Gamma^c_{15}$. Unlike Ge the leading absorption edge of Si rises sharply since the top of the valence band and the bottom of the conduction band are almost parallel along Λ. However, critical-point structure at 2.86 eV associated with the $L^v_{3'} \rightarrow L^c_1$ transition is not noticeable in the theoretical curve. Three small structures are found at 3.05, 3.23, and 3.73 eV; a major peak at 4.10 eV followed by a weak shoulder at 5.05 eV. The structure at 3.05 eV arises mainly from the $\Gamma^v_{25'} \rightarrow \Gamma^c_{2'}$ transition, while transitions along Δ ($\Delta^v_5 \rightarrow \Delta^c_1$ near X and $\Delta^v_5 \rightarrow \Delta^c_{2'}$ near Γ) are responsible for the one at 3.73 eV. The 3.23-eV structure appears to occur between the top of the valence band and the bottom of the conduction band in the vicinity of (4,4,3) and (3,3,0) in units of $\pi/4a$. A large region along Σ ($\Sigma^v_2 \rightarrow \Sigma^c_3$) contributes to the main peak at 4.10 eV although there is also some contribution from $\Delta^v_5 \rightarrow \Delta^c_{2'}$ near X. Similar to what we found for Ge, the shoulder beginning at 5 eV is attributed to the transitions $\Lambda^v_3 \rightarrow \Lambda^c_3$ near L, and also $\Delta^v_5 \rightarrow \Delta^c_{2'}$, with the sharp structure at 5.06 eV coinciding with the $L^v_{3'} \rightarrow L^c_3$ transition.

Note that the overall width of the theoretical ϵ_2 for Si is slightly larger than the experiment, a feature we found impossible to improve by either the lifetime or self-energy corrections. A value of 0.04 was chosen for λ to align the main peak around 4 eV, and 0.04 eV for $1/\tau$ to reproduce its width, but the leading absorption edge remains lower than experiment. Since the screened Coulomb interaction between the excited electron and the hole left behind would undoubtedly reduce the transition energy, our final $E1$ peak would lie lower in energy than the experiment unless the excitonic effect is dominated by the third structure (along Δ). Hanke and Sham reported[16] that the continuum-excitonic effect, which is dominant around the $E1$ position, arises from quite extended regions in the Brillouin zone and includes contributions from regions near the critical points Γ and L. Note that the differences in line shapes between our results and the experiments for Si is larger and more complicated than that of Ge whose transitions can be uniquely identified. In a study of the room-temperature derivative reflectivity spectra of Ge-Si alloys, Welkowsky and Braustein[26] show that the position of the $E1$ peak is a linear function of the Si concentration until approximately 78 at % Si, when the slope suddenly changed. This was interpreted as an indication that the Λ transition, which is responsibel for $E1$ peak in Ge, is no longer the origin of the Si transition.

Our results within the one-electron picture agree very well with the earlier empirical pseudopotential calculation.[7] Slight shifts in the peak positions are understandable since we based our *ab initio* calculation on the local-density-functional formalism while their energies were adjusted empirically to reproduce the experiments. Both calculations show significant deficits in the oscillator strength of the $E1$ peak compared to experiments. The height of their main $E2$ optical peak, 47, agrees very well with our result of 48. At energies above the $E2$ peak we found our ϵ_2, corrected for lifetime and self-energy effects, lies higher than experiment until approximately 8 eV, where the situation is reversed. Louie *et al.*[7] have demonstrated that local-field effects will improve the agreement of our result with experiment in these regions.

3. GaP and GaAs

We shall combine our discussions on GaP and GaAs here since their band structures and ϵ_2 spectra are extremely similar. In excellent agreement with recent results of energy derivative reflectance spectra of the 20-eV transition from the Ga $3d$ core hole excitation to the lower conduction bands in $GaAs_{1-x}P_x$ alloys,[27] we found the conduction minimum at X lies below L for GaP (giving rise to an indirect band gap $\Gamma^v_{15} \rightarrow \Delta^c_1$ of 1.80 eV) and above L for GaAs (with a direct band gap of 1.21 eV at Γ). However, this reverse ordering between the lowest L and X point conduction-band states for these two compounds introduces no qualitative difference in the low-energy optical transitions. The theoretical ϵ_2 due to interband transitions are shown as dotted lines in the middle of Fig. 1 for GaP and GaAs. The onset of the absorption edge occurs at 2.05 and 1.21 eV, respectively, which corresponds to the $\Gamma^v_{15} \rightarrow \Gamma^c_1$ transitions. The intensity increases slowly as the band gaps open up away from Γ; around one-fourth of the way to L along the Λ direction the valence and conduction bands become parallel to each other and the oscillator strength begins to rise sharply at 3.05 and 2.49 eV. At the top of the $E1$ peak at 3.52 and 2.90 eV, contributions

arise from (4,4,3) to (2,2,0) to (2,1,1) in units of $\pi/4a$ in the Brillouin zone. The main $E2$ peak arises from transitions along the Δ direction which also extend near the outer portions of the Brillouin zone toward the Σ direction, including the critical points $X_5^v \rightarrow X_1^c$ at 4.51 and 4.25, $X_5^v \rightarrow X_3^c$ at 4.81 and 4.51, and $K_2^v \rightarrow K_1^c$ at 4.64 and 4.36 eV, respectively, for GaP and GaAs. Finally, the last shoulder corresponds to the $\Lambda_3^v \rightarrow \Lambda_3^c$ transition, with the sharp structures at 6.20 and 6.27 eV coinciding with the $L_3^v \rightarrow L_3^c$ transition.

We found that a value of 0.08 and 0.06 for λ gave the best fit to the position of the main optical peak in GaP and GaAs, respectively, and $1/\tau = 0.1$ eV reproduces the corresponding width rather well. The resulting oscillator stength of the theoretical $E1$ peak is slightly stronger in GaAs than in GaP which is consistent with the comparison between Ge and Si since GaAs (Ge) is less covalent than GaP (Si). Comparison of the experimental results for GaAs and Ge,[1] however, show that the $E1$ peak is almost as high as the $E2$ peak in GaAs in contrast to the results for Ge, where the $E1$ peak is much weaker. Thus, excitonic effects in GaAs turn out to be surprisingly strong compared to those in Ge.

4. *ZnS and ZnSe*

The low-energy optical spectra for ZnS and ZnSe (bottom panel of Fig. 1) are very similar to those of GaP and GaAs (middle panel). Therefore we will not repeat our discussion other than mentioning the location of the interband optical transitions: The absorption edge occurs at 1.83 (2.26) eV, the $E1$ peak at 4.02 (4.76) eV, and the main $E2$ peak at 5.53 (6.20) eV for ZnSe (ZnS), respectively. The shoulder above the main optical peak in GaP and GaAs, which arises mainly from the $\Lambda_3^v \rightarrow \Lambda_3^c$ transition, is split into three structures here because the Γ_{15}^c and X_3^v levels are raised relative to the valence-band maximum as the system becomes more ionic in ZnS and ZnSe. Thus, the valence and conduction bands are more or less parallel to each other away from the Λ direction as well. The first weak shoulder at 6.14 (6.95) eV in ZnSe (ZnS) lies very close to the $\Gamma_{15}^v \rightarrow \Gamma_{15}^c$ transition at 5.86 (7.03) eV and is dominated by a region near the Δ direction. The second structure at 7.08 (7.79) eV is due to a volume effect which extends over the intermediate portion of the Brillouin zone, and the third one at 7.56 (8.30) eV is mainly centered around the $L_3^v \rightarrow L_3^c$ transition.

The overall agreement with experiments[2,3] (dashed lines) was improved significantly when the following parameters were used for the lifetime: $1/\tau = 0.08$ (0.05) eV, and the self-energy correction: $\lambda = 0.15$ (0.12) for ZnSe (ZnS), respectively. However, the leading absorption edge remains substantially lower than the experiments for all zinc-blende materials studied. Presumably this is due to the large difference in the spatial character of the predominantly s-like Γ_1 state (localized around the nucleus) and the rest of the antibonding p state, making the approximation that $\lambda_n(\vec{k})$ in Eq. (3) is independent of the band index n and wave vector $\vec{k}$ less accurate. As we found for Si and Ge, the theoretical $E1$ structure is slightly more pronounced in the less covalent ZnSe than in ZnS, although the experimental $E1$ structure is much stronger in ZnS. Thus, the excitonic effects are more important in ZnS.

B. $\epsilon_1(\omega)$

The real part of the dielectric constant $\epsilon_1(\omega)$ calculated by Kramers-Kronig transforming $\epsilon_2(\omega)$ before (dotted lines) and after (solid lines) including lifetime and self-energy corrections are shown in Fig. 2 where they are compared with experiment[1-3] (dashed lines). In general, we found qualitatively good agreement with experiment although there are some quantitative differences in the intensity and the

TABLE I. Comparison of the interband contribution to the optical dielectric constant with experiments.

Material	Theory	Experiment
Si	11.7	11.7[a]
		12.0[b]
Ge	16.0	15.8[a]
		16.0[b]
GaP	9.4	9.1[c]
GaAs	10.9	10.9[d]
ZnS	5.5	5.2[e]
ZnSe	6.6	5.9[f]

[a]Reference 28.
[b]Reference 29.
[c]Reference 30.
[d]Reference 31.
[e]Reference 32.
[f]Reference 33.

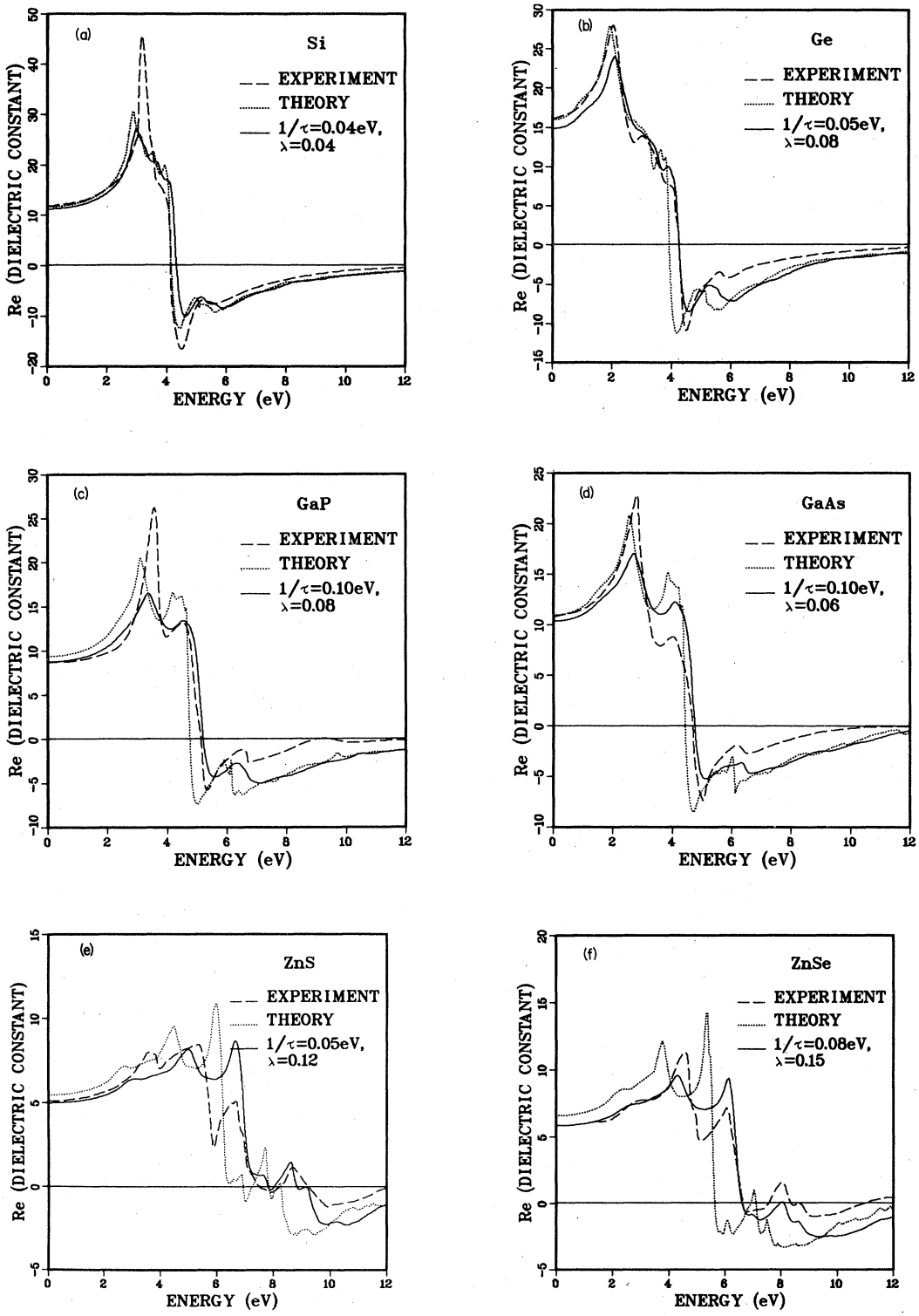

FIG. 2. Real part of the dielectric constant. The experimental results (dashed lines) are from Ref. 1 for Ge, Si, GaP, and GaAs, Ref. 2 for Zns, and Ref. 3 for ZnSe. The dotted lines are interband contributions to Eq. (1), while the solid lines include additional lifetime-broadening and self-energy corrections as indicated in each figure and discussed in the text.

position of the spectra due to many-body effects not included in our calculations. As can be seen from Table I our static dielectric constants $\epsilon(0)$ due to interband transitions agree extremely well with the experiments[28–33] after they are corrected for electron-phonon interactions. They are, however, subject to the following modifications: (1) The local-density-functional formalism has the tendency of underestimating the optical band gaps which will shift the oscillator strength to lower energy in ϵ_2 and enhance the static dielectric constant; (2) Both Hanke and Sham[16] and Louie *et al.*[7] found that the local-field effect reduced the value of $\epsilon(0)$ for Si; (3) the excitonic effect, which will move the oscillator strength from higher energy to the $E1$ peak and lower its transition energy, will undoubtedly raise $\epsilon(0)$ as Hanke and Sham have found for Si.

Based on an initial value of 9.85 for $\epsilon(0)$ of Si, Hanke and Sham[16] have investigated the possibility of using the local-density approximation to account for many-body effects in Si. After correcting for excitonic and local-field effects they found too low a value (8.9) for $\epsilon(0)$ compared to the experimental value[28] of 11.7 and concluded that the local-density scheme cannot properly account for the electron-hole attraction in a covalently bonded crystal. To be consistent, however, they should really start from our value of 11.7 for Si which was calculated self-consistently within the same local-density formalism. With corrections of either -1.1 (Louie *et al.*[7]) or -1.85 (Hanke and Sham[16]) for the local-field effect, and 0.9 for the local-density excitonic effect found by Hanke and Sham, our result would yield a value of 11.5 or 10.75 which agrees with experiment (11.7) even better than Hanke and Sham's value of 10.4. Thus, a rather different conclusion may be drawn depending on the choice of the starting one-electron energy bands. Furthermore, there are important fundamental differences between the nonlocal Hartree-Fock exchange potential and the local-density-functional exchange-correlation potential. The Hartree-Fock potential tends to overestimate the measured optical band gaps while the local density theory underestimates them. Thus, the corresponding many-body corrections to the two potentials may be opposite in sign. We emphasize that many-body corrections developed for a Hartree-Fock potential are not transferable to a local-density band structure, and vice versa.

It is of interest to note that the first peak in $\epsilon_1(\omega)$ coincides with the transition at L between the top of the valence band and the bottom of the conduction band which was not noticeable in $\epsilon_2(\omega)$, and the energy where $\epsilon_1(\omega)=0$ is very close to the maximum of the $E2$ peak in $\epsilon_2(\omega)$. At high energy, where the theoretical $\epsilon_2(\omega)$ is consistently lower than experiment, we found our $\epsilon_1(\omega)$ more negative. Although these discrepancies appear to be unimportant [the absolute magnitude of $\epsilon(\omega)$ is very small], they have an adverse effect on the energy-loss spectrum and reflectance at high energy.

C. Energy-loss spectra

Figure 3 compares our energy-loss spectra $-\mathrm{Im}(1/\epsilon)$ with experiment. The main feature is the plasmon peak whose position corresponds to $\epsilon_1(\omega)=0$, provided $\epsilon_2(\omega)$ is reasonably smooth in these regions. In general, we found rather good agreement with experiment as to peak position, but the peak height is overestimated by more than a factor of 2. At an energy of more than 15 eV above the top of the valence band one may question the variational flexibility of our LCAO basis set. Comparison of our energy-loss spectrum for Si with earlier studies by Louie *et al.*[7] using pseudopotentials and a plane-wave basis set turns out to be extremely encouraging. Our plasma peak height of 7.4 agrees very well with their value of 7.2, although the experimental value is 1.9. Our peak position 17.0 eV is also in good agreement with their value of 18.1 eV; the experimental result is 16.2 eV. Significant improvement was found by Louie *et al.* when the local-field correction was included. Their theoretical peak height is reduced to 3.3, and the peak position is shifted to 16.9 eV. Hanke and Sham[16] noted that they found that the excitonic effect gave a further enhancement of the plasma peak strength. As we mentioned before, there may be too much difference between their starting one-electron $\epsilon_2(\omega)$ and that of either Louie *et al.* or our results, especially at this high energy, to be too conclusive about this point.

Another interesting point raised by Bardasis and Hone[34] is that the dominant scattering process for a high-energy conduction electron is the Auger-type transitions involving two electrons that need not conserve momentum. Such effects may be responsible in part for the discrepancy between theory and experiment at high energy.

D. Reflectivity

The theoretical and experimental[1–3] reflectivity appears in Fig. 4. Below 7 eV the theoretical

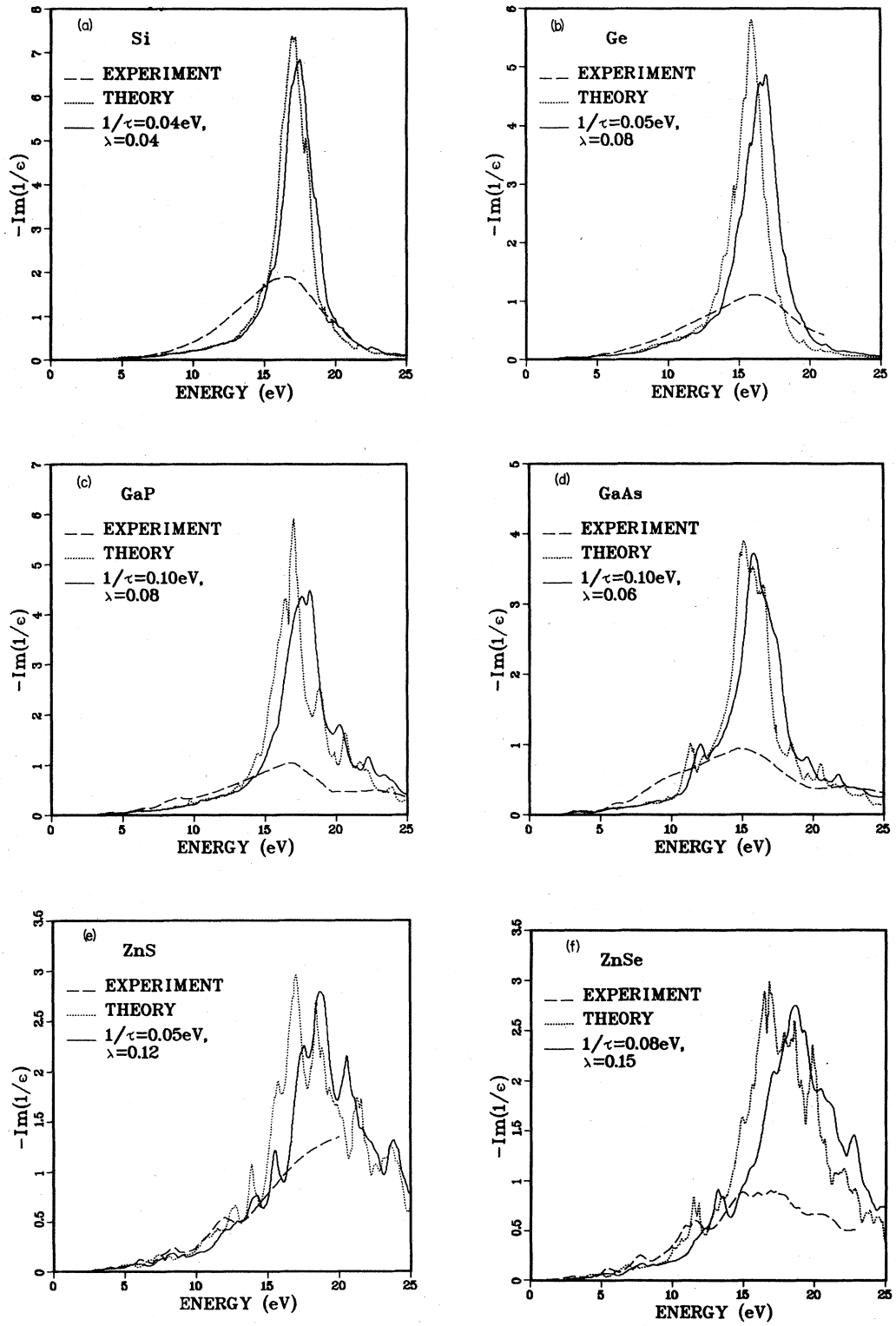

FIG. 3. Energy-loss spectra. The experimental results (dashed lines) are from Ref. 1 for Ge, Si, GaP, and GaAs, Ref. 2 for ZnS, and Ref. 3 for ZnSe. The dotted lines arise from interband contributions, while the solid lines include additional lifetime-broadening and self-energy corrections as indicated in each figure and discussed in the text.

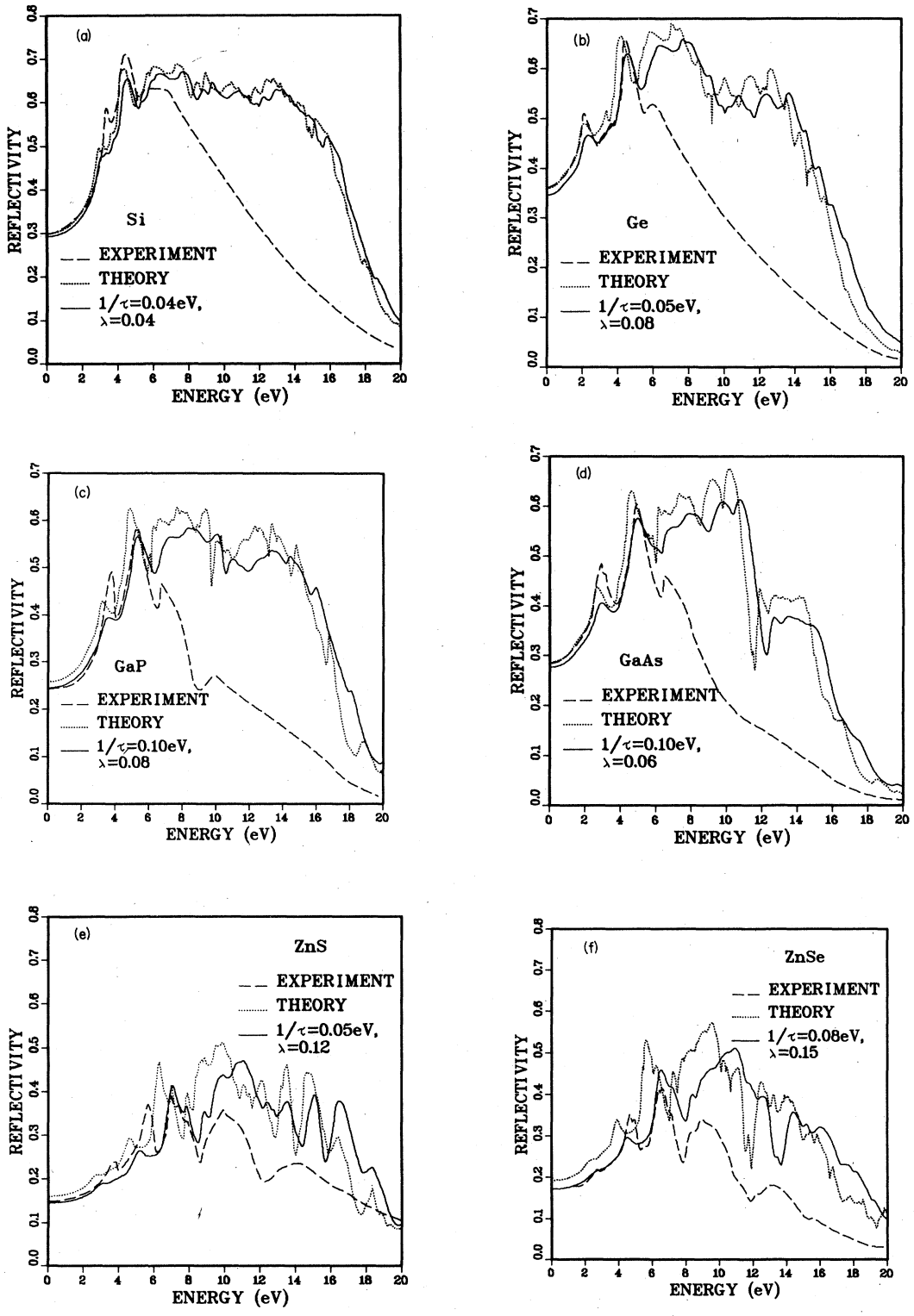

FIG. 4. Reflectivity spectra. The experimental results (dashed lines) are from Ref. 1 for Ge, Si, GaP, and GaAs, Ref. 2 for ZnS, and Ref. 3 for ZnSe. The dotted lines arise from interband contributions, while the solid lines include additional lifetime-broadening and self-energy corrections as indicated in each figure and discussed in the text.

results, including lifetime and self-energy corrections, have the same shape as the experiments and the peak positions agree, but the amplitudes differ as was found in $\epsilon_2(\omega)$. A rather surprising result is the *large* discrepancy (more than 50%) found at high energies. This problem was noted in earlier empirical pseudopotential calculations[6] although their energy ranges were limited by approximating their theoretical $\epsilon_2(\omega)$, with a tail function beginning around 10 eV. In view of the good agreement with Louie *et al.*[7] for the energy-loss spectrum of Si, we believe our results reflect a genuine deficiency of the one-electron picture in describing the reflectivity spectra at high energies.

IV. CONCLUSION

The interband optical properties of Si, Ge, GaP, GaAs, ZnS, and ZnSe have been investigated. Our calculations differ from previous studies using the empirical pseudopotential method in that it is a first-principles procedure with the lattice constant being the only experimental input, and the local-density approximation the only theoretical assumption. Thus, a comparison of our results with experiments reflects, without any ambiguity, the many-body effects not included in the Koopman's theory for the optical spectra. Based on the Sham-Kohn local-density theory of single-particle-like excitations,[24] we have demonstrated how the line shapes and positions of the optical spectra can be improved. A more sophisticated theory involving solutions to the two-particle Green's function for the electron-hole interaction has recently become available.[16] Since a detailed numerical assessment depends critically on the accuracy of the one-electron energy bands, the present papers should serve as an ideal starting point for further investigations of the excitonic and local-field effects in covalent semiconductors.

ACKNOWLEDGMENTS

We thank D. A. Papaconstantopoulos and W. E. Pickett for helpful discussions and comments on the manuscript, and Andrew Koppenhaver for technical assistance. This work was supported by the Office of Naval Research, Contract No. N00014-79-WR-90028.

[1]H. R. Philipp and H. Ehrenreich, Phys. Rev. 129, 1550 (1963).
[2]M. Cardona and G. Harbeke, Phys. Rev. 137, A1467 (1965).
[3]J. L. Freeouf, Phys. Rev. B 7, 3810 (1973).
[4]J. R. Chelikowsky and M. L. Cohen, Phys. Rev. B 14, 556 (1976); 10, 5025 (1974).
[5]R. R. I. Zucca, J. P. Walter, Y. R. Shen, and M. L. Cohen, Solid State Commun. 8, 627 (1970).
[6]J. P. Walter, M. L. Cohen, Y. Petroff, and M. Balkanski, Phys. Rev. B 1, 2661 (1970).
[7]S. G. Louie, J. R. Chelikowsky, and M. L. Cohen, Phys. Rev. Lett. 34, 155 (1975).
[8]W. D. Grobman, D. E. Eastman, and J. L. Freeouf, Phys. Rev. B 12, 4405 (1975).
[9]T. C. Collins, D. J. Stukel, and R. N. Euwema, Phys. Rev. B 1, 724 (1970).
[10]D. J. Stukel, R. N. Euwema, T. C. Collins, F. Herman, and R. L. Kortum, Phys. Rev. 179, 740 (1969).
[11]J. C. Phillips, Phys. Rev. 136, A1705 (1964).
[12]B. Velicky and J. Sak, Phys. Status Solidi 16, 147 (1966).
[13]R. R. I. Zucca and Y. R. Shen, Phys. Rev. B 1, 2668 (1970).
[14]J. E. Rowe, F. H. Pollak, and M. Cardona, Phys. Rev. Lett. 22, 933 (1969).
[15]K. L. Shaklee, J. E. Rowe, and M. Cardona, Phys. Rev. 174, 828 (1968).
[16]W. Hanke and L. J. Sham, Phys. Rev. B 21, 4656 (1980).
[17]P. Hohenberg and W. Kohn, Phys. Rev. 136, B864 (1964).
[18]W. Kohn and L. J. Sham, Phys. Rev. 140, A1133 (1965).
[19]C. S. Wang and J. Callaway, Comput. Phys. Commun. 14, 327 (1978).
[20]E. Wigner, Phys. Rev. 46, 1002 (1934).
[21]D. J. Chadi and M. L. Cohen, Phys. Rev. B 8, 5747 (1973).
[22]D. Jepsen and O. K. Anderson, Solid State Commun. 9, 1763 (1971); G. Lehman and M. Taut, Phys. Status Solidi 54, 469 (1972).
[23]J. F. Janak, A. R. Williams, and V. L. Moruzzi, Phys. Rev. B 11, 1522 (1975).
[24]L. J. Sham and W. Kohn, Phys. Rev. 145, 561 (1966).
[25]L. Hedin and S. Lundqvist, Solid State Phys. 23, 1 (1969).
[26]M. Welkowsky and R. Braunstein, Phys. Rev. B 5, 497 (1972).
[27]S. M. Kelso, D. E. Aspnes, C. G. Olson, D. W. Lynch, and D. Finn, Phys. Rev. Lett. 45, 1032 (1980).

[28]C. Kittel, *Introduction to Solid State Physics* (Wiley, New York, 1976), p. 309.
[29]W. A. Harrison *Electronic Structure and the Properties of Solids* (Freeman, San Francisco, 1980), p. 114.
[30]A. S. Barker, Jr., Phys. Rev. 165, 917 (1968).
[31]M. Hass and B. W. Henvis, J. Phys. Chem. Solids 23, 1099 (1962).
[32]S. J. Czyzah, W. M. Baker, R. C. Crane, and J. B. Howe, J. Opt. Soc. Am. 47, 240 (1957).
[33]D. T. F. Marple, J. App. Phys. 35, 539 (1964).
[34]A. Bardasis and D. Hone, Phys. Rev. 153, 849 (1967).